Liquid crystalline assemblies of ordered gold nanorods

Nikhil R. Jana,[a] Latha A. Gearheart,[a] Sherine O. Obare,[a] Christopher J. Johnson,[b] Karen J. Edler,[c] Stephen Mann*[b] and Catherine J. Murphy*[a]

[a]Department of Chemistry and Biochemistry, University of South Carolina, Columbia, SC 29208, USA. E-mail: murphy@mail.chem.sc.edu
[b]School of Chemistry, University of Bristol, Bristol, UK BS8 1TS. E-mail: s.mann@bristol.ac.uk
[c]Department of Chemistry, University of Bath, Claverton Down, Bath, UK BA2 7AY

Gold nanorods have been prepared in aqueous solution using a seed-mediated growth approach in the presence of surfactant. We observe the formation of liquid crystalline phases in concentrated solutions of high aspect ratio (13–18) gold nanorods by polarizing microscopy, transmission electron microscopy, and small angle X-ray scattering. These phases, which are stable up to 200 °C, exhibit concentration-dependent orientational order.

Introduction

The multiscale ordering of nanoparticles is essential for the integration and application of nanomaterials in many macroscopic devices.[1,2] Current methods for assembling gold nanoparticle superstructures involve capillary forces,[3,4] molecular[5,6] and biomolecular[7–9] cross-linking, and template-directed patterning[10,11] In general, these approaches produce aggregates that are either supported on substrates or phase-separated from solution in the form of colloidal crystals or precipitates; in contrast, there are few examples of dispersed nanoparticle-based ordered assemblies.[12] Lyotropic liquid crystalline phases of colloidal rods and platelets have long been predicted[13] and are now being experimentally discovered.[14–16] Such systems could provide the basis for a general route to multiscale ordering of metallic nanoparticles for device incorporation. Recent theoretical and experimental studies have shown that ordered liquid crystalline phases can form in concentrated dispersions of anisotropic colloidal particles.[14–22] These superstructures are thermodynamically stable due to a gain in translational entropy that overrides the loss of orientational entropy associated with particle alignment.[13] However, the number of practical examples is currently low because of the difficulty of synthesizing populations of particles with homogeneous shape and size. For example, 2-D smectic phases are predicted to be unstable for polydispersities greater than 18%.[20] Recently, several examples of rod-shaped metallic[23–27] and semiconductor[28] nanoparticles have been reported; these nanorods can be self-assembled into ordered 2-D superstructures by solvent evaporation[29] or Langmuir–Blodgett techniques,[30] or into colloidal aggregates using surface-adsorbed oligonucleotides and DNA hybridization.[31] In this paper, we employ a three-step seeding growth procedure[25] to produce surfactant-coated gold nanorods with low polydispersity (14%) and high aspect ratio (13–18; mean length = 200–290 nm) that spontaneously self-assemble in concentrated solutions to produce liquid crystals based on ordered arrays of metallic nanoparticles.

Experimental

Gold nanorods were prepared in water as described previously.[25] Briefly, a 20 mL gold seed solution containing 2.5×10^{-4} M $HAuCl_4$ and 2.5×10^{-4} M trisodium citrate was prepared in a conical flask. Next, 0.6 mL of ice cold 0.1 M $NaBH_4$ solution was added to the reaction mixture in a single portion while stirring. The solution turned pink immediately after addition of the $NaBH_4$, indicating particle formation. The particles in this solution were used as seeds within 2–5 h after preparation. The average particle size measured from the transmission electron micrograph was 3.5 ± 0.7 nm. 9 mL of 0.1 M cetyltrimethylammonuim bromide (CTAB) were placed in each of three test-tubes (labeled 1, 2, and 3 respectively). 0.25 mL of a 10^{-2} M $HAuCl_4$ stock solution and 0.05 mL of a 0.01 M ascorbic acid solution were added to each test-tube. Next, 1 mL of gold seed solution was added to test-tube 1. The solution was rapidly stirred for approximately 30 s, then 1 mL of the contents of tube 1 were added to the contents of tube 2. Tube 2 was stirred for 30 s, then 1 mL of the tube 2 solution was added to the contents of tube 3. Tube 3 was stirred for 30 s and allowed to stand overnight undisturbed, allowing the rods to form. Excess CTAB was removed from the nanoparticles by centrifuging tube 3 at 2000 rpm for 30 min at room temperature. The supernatant, containing CTAB, was removed, leaving behind gold rods that were re-dispersed in 1 mL of water. The aspect ratio of the resulting nanorods was 13–18.

Liquid crystalline assemblies were observed in the range 1–100 mM CTAB. Samples were prepared for optical microscopy by concentrating 5 µL of concentrated Au nanorod solution on a glass slide by slow partial evaporation. A PZO Model ZM 100 T optical microscope was used to acquire optical microscopy images for both liquid crystalline Au nanorod assemblies and CTAB. TEM images were recorded from dilute and concentrated aqueous suspensions of gold nanorods that were dried by slow evaporation. A JEOL 1200EX analytical electron microscope operating at 80 kV accelerating voltage was used.

SAXS experiments were performed on concentrated and diluted dispersions of gold nanorods in 1.5 mm diameter X-ray glass capillary tubes using beamline BM26B at the ESRF[32] with a beam energy of 15 keV. The data were calibrated against silver behenate, and fitted within the IGOR Pro platform (Wavemetrics, Inc., Lake Oswego, OR, USA). The structural models used were modified from those written by the 'SANS group' at the NIST Centre for Neutron Research (http://www.ncnr.nist.gov/programs/sans/).[33] The fits used calculated values for the scattering contrast between the gold particles, the surfactant layer, and the solvent (water), and the length of the particles was set to that measured by TEM (200 nm) as the fit is not particularly sensitive to the length of

highly elongated particles. Polydispersity in the radius of the nanorods was incorporated based on particle size distributions measured by TEM. As the nanoparticle sample contained $\sim 3\%$ impurity of spheroidal nanoparticles, a contribution from a small proportion of prolate ellipses with a major to minor axis ratio of 0.83 (averaged from TEM images) and surfactant coating equal in thickness to that of the rods was included in the model.

Results

The gold nanorods, which originate from the surfactant-mediated growth of penta-twinned primary crystallites,[34] were concentrated and separated from any spherical nanoparticles by centrifugation. Thermogravimetric analysis showed that $\sim 20\%$ of the total mass of the nanorods was associated with the surfactant, cetyltrimethylammonium bromide (CTAB). This is significantly larger than calculated for monolayer coverage (3 wt%) on the basis of particle surface area, and indicates that the nanorods are covered with multiple CTAB layers, as also shown by previous spectroscopic studies.[35] The presence of the surfactant coating was of key importance not only for hydrophilic stabilization of the nanorods in water, but also for controlling long range self-assembly in concentrated dispersions. For example, we found that the optimum conditions required for *in situ* liquid crystalline ordering involved redispersing the nanorods in 1–100 mM CTAB after separating the rods from spheres by centrifugation. Above this surfactant concentration, the nanorods precipitated instantaneously and could not be redispersed to image in the electron microscope. Below this CTAB concentration, the nanorods could not be redispersed in water. Although this situation has not been fully explored, we believe these effects mean that a surfactant is required to counteract them, since addition of ~ 1 mM NaCl precipitates the nanorods.

In general, the aspect ratio 18 nanorod solutions were dark brown in color (when concentrated) and had a weak absorbance maximum in the visible at ~ 530 nm, in addition to a near-infrared absorbance at ~ 1700 nm.[25] Thin films of concentrated dispersions supported on glass slides showed iridescent droplets ~ 0.1 mm in diameter under polarizing light microscopy (Fig. 1). The observed textures were indicative of localized regions of liquid crystalline ordering and are similar to nematic droplets observed in boehmite nanoneedle solutions.[14] Significantly, the liquid crystalline droplets were stable up to 200 °C in air, after which the surfactant began to degrade, although the nanorods remained unchanged in size and shape.
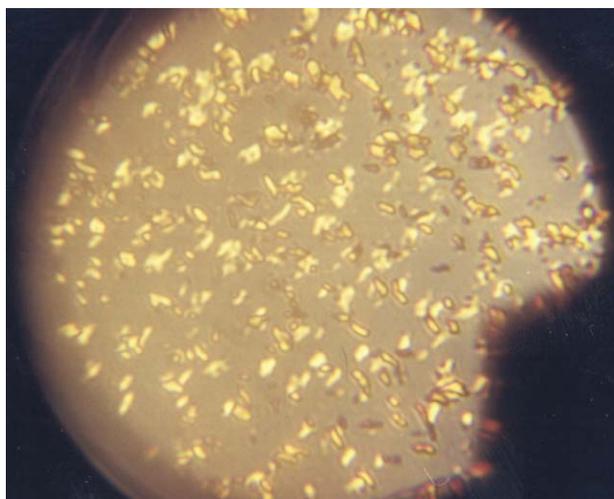
Fig. 1 Polarizing light microscope image of 5–10 wt% concentrated gold nanorods in aqueous solution placed on a microscope slide. The image was taken at 100 × magnification. The average feature size is ~ 0.1 mm.
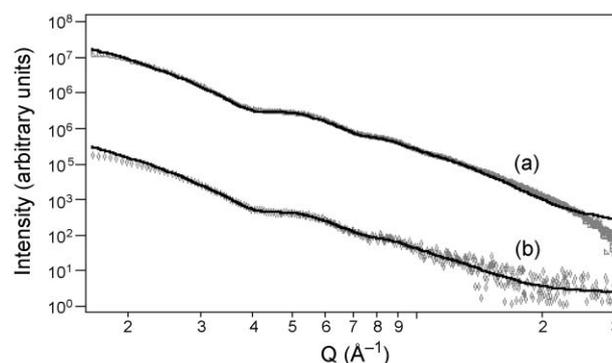
Fig. 2 Small angle X-ray scattering patterns for (a) the concentrated solution of nanorods (~ 5–10 wt% solids) and (b) the dilute solution of nanorods (by a factor of ~ 1000). $Q = 4\pi \sin\theta/\lambda$, where 2θ is the scattering angle and λ the X-ray wavelength. Symbols represent data points, the solid lines are the fits to the data.

Similar experiments with concentrated surfactant solution alone showed much smaller 'speckles' in the polarizing microscope and no liquid crystalline textures.

Small angle X-ray scattering (SAXS) experiments were undertaken to determine the extent of long range ordering in concentrated (~ 5–10 wt% solids) and diluted (by a factor of ~ 1000) dispersions of the gold nanorods. The corresponding scattering curves are shown in Fig. 2. Both curves show ripples in the scattered X-ray intensity due to particle shape and interparticle interactions. The data were fitted to a model consisting of core–shell cylinders stacked with a Gaussian distribution of interparticle distances using a method of non-linear least-squares fitting. The fitting parameters included the radius of the nanorods, number of particles in a stack, width of the Gaussian distribution of interparticle distances in the stack, surfactant layer thickness, and major radius of the elliptical impurities (see Experimental methods). Attempts to fit the SAXS data to isolated rods failed; rod stacks were required. The fits suggest that the concentrated solutions contained self-assembled stacks of ~ 200 nanorods, each of which had a surfactant coating 3.9 nm in thickness, consistent with a CTAB bilayer. In contrast, smaller clusters of ~ 30 rods were present in the more dilute sample. The width of the Gaussian distribution of spacings between the particle centers was an order of magnitude narrower in the concentrated dispersions compared to the dilute dispersions, consistent with more dense arrays in the concentrated dispersions and a high degree of disorder in the dilute dispersions. No evidence for hexagonal phases was found, under our conditions.

TEM images of air-dried dispersions prepared at low nanorod concentrations ($<1\%$ by weight, including surfactant) showed mainly discrete nanoparticles [Fig. 3(a)]. Some short range order involving side-on, end-to-side, or end-to-end aggregation was observed, presumably due to capillary forces associated with the drying process.[29] At high nanorod concentrations (~ 5–10 wt%), in contrast, microscopic smectic-like arrays of closely packed nanorods were observed [Fig. 3(b)]. The arrays consisted of nanorods that were aligned parallel to each other in micrometre-sized rows, which, in turn, were stacked laterally to produce the higher order superstructure. Such structures were observed predominantly at the edges of dried droplets (apparent as brown rings on visual inspection of the TEM grid), suggesting that capillary forces were responsible for the smectic-like organization. In contrast, other areas of the TEM grid showed a predominance of micrometre-long rows of ordered nanorods [Fig. 3(c)], which probably correspond more closely to the *in situ* organization of the nanorods within the concentrated dispersion. We estimate tens of rods assemble in vertical stacks, while ~ 100 stacks assemble into rows, in reasonable agreement with the SAXS data, given the
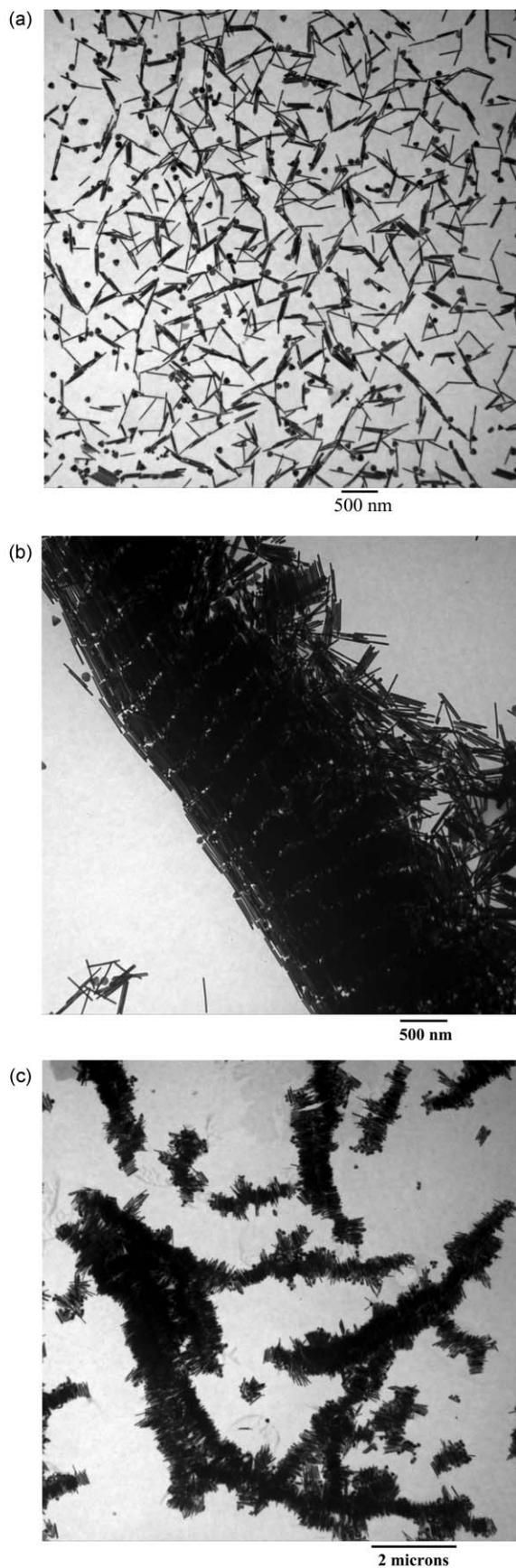
large uncertainties in this fitted parameter. The smectic-like phase presumably arises from secondary ordering of the preformed linear stacks on the TEM grid during drying.

Discussion

El-Sayed *et al.* have reported that gold nanorods of aspect ratio 4.6, coated with two different cationic surfactants, assemble into higher order structures upon concentration from aqueous solution.[29] Our results with higher aspect ratio nanorods are consistent with this and indicate that surfactant-mediated interactions between gold nanorods of uniform shape and size can give rise to ordered liquid crystalline arrays in concentrated suspensions. Multilayers of surface-adsorbed cationic surfactants such as CTAB can induce a remarkable degree of self-ordering of spherical gold nanoparticles, due to a balance between short range electrostatic repulsion and interchain attraction.[36] Moreover, interdigitation of surfactant chains on specific faces of prismatic nanocrystals can give rise to ordered single chains of other ($BaCrO_4$) nanoparticles.[12] For the gold nanorods described here, liquid crystalline arrays were only routinely observed in aqueous solutions containing the appropriate concentration range of CTAB, suggesting that interactions between surfactant molecules in solution with surface-adsorbed amphiphiles were important aspects of the assembly process. The hydrophilic nature of the gold nano-particles prior to assembly indicates that the surfactant molecules in the outer layer of the surface coating are oriented with their cationic headgroups exposed to the solvent. However, as the surfactant-coated nanorods approach each other in solution, expulsion of the outermost 'cationic head out' CTAB molecules and their associated counterions could result in the formation of hydrophobic nanorods in which the remaining CTAB hydrophobic tails face the solvent; thus, the resulting nanorods spontaneously self-assemble in a side-on fashion to minimize the unfavorable hydrophilic–hydrophobic interactions with water and promote interdigitation of the surfactant tails.

Finally, we note that alignment of gold nanorods coated with an anionic polymer has been recently achieved in aqueous solution by the application of electric fields[37] and in thin stretched polymer films,[38] and that the corresponding absorbance spectra only show the longitudinal or transverse plasmon band when the absorbing light is polarized parallel or perpendicular, respectively, to the nanoparticle long axis. The ability to spontaneously self-assemble metallic nanoparticle-based liquid crystals in solution, as described here, could offer significant technological advantages. For example, the combination of liquid crystal nanorod ordering with electric field-induced switching could be a promising approach for optoelectronic applications.

Acknowledgements

References

1 C. P. Collier, T. Vossmeyer and J. R. Heath, *Annu. Rev. Phys. Chem.*, 1998, **49**, 371–404.
2 A. N. Shipway, E. Katz and I. Willner, *ChemPhysChem.*, 2000, **1**, 18–52.
3 S. R. J. Oliver, N. Bowden and G. M. Whitesides, *J. Colloid Interface Sci.*, 2000, **224**, 425–428.
4 Z. L. Wang, *Adv. Mater.*, 1998, **10**, 13–30.

Fig. 3 Transmission electron micrographs showing concentration-dependent ordering of gold nanorods: (a) <1 wt% dispersion, showing isolated nanorods; some spherical particles are still present, even after centrifugation; (b) ~5–10 wt% dispersion, showing smectic-like arrays; (c) ~5–10 wt% dispersion, showing linear stacks of gold nanorods.

5   M. Brust, D. Bethell, D. J. Schiffrin and C. J. Kiely, *Adv. Mater.*, 1995, **7**, 795–797.
6   R. P. Andres, *Science*, 1996, **273**, 1690–1693.
7   C. A. Mirkin, R. L. Letsinger, R. C. Mucic and J. J. Storhoff, *Nature*, 1996, **382**, 607–609.
8   S. Mann, W. Shenton, M. Li, S. Connolly and D. Fitzmaurice, *Adv. Mater.*, 2000, **12**, 147–150.
9   A. P. Alivisatos, K. P. Johnsson, X. Peng, T. E. Wilson, C. J. Loweth, M. P. Bruchez, Jr. and P. G. Schultz, *Nature*, 1996, **382**, 609–611.
10 S. Dieluweit, D. Pum and U. B. Sleytr, *Supramol. Sci.*, 1998, **5**, 15–19.
11 S. R. Hall, W. Shenton, H. Engelhardt and S. Mann, *ChemPhysChem.*, 2001, **3**, 184–186.
12 M. Li, H. Schnablegger and S. Mann, *Nature*, 1999, **402**, 393–395.
13 L. Onsager, *Ann. N. Y. Acad. Sci.*, 1949, **51**, 627–659.
14 J.-C. P. Gabriel and P. Davidson, *Adv. Mater.*, 2000, **12**, 9–20.
15 P. Davidson, J.-C. Gabriel, A. M. Levelut and P. Batail, *Europhys. Lett.*, 1993, **21**, 317–322.
16 A. S. Sonin, *J. Mater. Chem.*, 1998, **8**, 2557–2574.
17 D. Frenkel, H. N. W. Lekkerkerker and A. Stroobants, *Nature*, 1988, **332**, 822–823.
18 M. Adams, Z. Dogic, S. L. Keller and S. Fraden, *Nature*, 1998, **393**, 349–352.
19 F. M. van der Kooij and H. N. W. Lekkerkerker, *J. Phys. Chem. B*, 1998, **102**, 7829–7832.
20 M. A. Bates and D. Frenkel, *J. Chem. Phys.*, 1998, **109**, 6193–6199.
21 F. M. van der Kooij, K. Kassapidou and H. N. W. Lekkerkerker, *Nature*, 2000, **406**, 868–871.
22 S. Kwan, F. Kim, J. Akana and P. Yang, *Chem. Commun.*, 2001, 447–448.
23 Y. Y. Yu, S. S. Chang, C. L. Lee and C. R. C. Wang, *J. Phys. Chem. B*, 1997, **101**, 6661–6664.
24 M. P. Pileni, B. W. Ninham, T. Gulik, J. Tanori, I. Lisieki and A. Filankembo, *Adv. Mater.*, 1999, **11**, 1358–1362.
25 N. R. Jana, L. Gearheart and C. J. Murphy, *J. Phys. Chem. B*, 2001, **105**, 4065–4067.
26 N. R. Jana, L. Gearheart and C. J. Murphy, *Chem. Commun.*, 2001, 617–618.
27 V. F. Puntes, K. M. Krishnan and A. P. Alivisatos, *Science*, 2001, **291**, 2115–2117.
28 X. G. Peng, L. Manna, W. D. Yang, J. Wickham, E. Scher, A. Kadavanich and A. P. Alivisatos, *Nature*, 2000, **404**, 59–61.
29 B. Nikoobakht, Z. L. Wang and M. A. El-Sayed, *J. Phys. Chem. B*, 2000, **104**, 8635–8640.
30 F. Kim, S. Kwan, J. Akana and P. Yang, *J. Am. Chem. Soc.*, 2001, **123**, 4360–4361.
31 E. Dujardin, L.-B. Hsin, C. R. C. Wang and S. Mann, *Chem. Commun.*, 2001, 1264–1265.
32 W. Bras, *J. Macromol. Sci. Phys.*, 1998, **37**, 557–565.
33 D. L. Ho, R. M. Briber and C. J. Glinka, *Chem. Mater.*, 2001, **13**, 1923–1931.
34 C. J. Johnson, E. Dujardin, S. A. Davis, C. J. Murphy and S. Mann, *J. Mater. Chem.*, 2002, **12**, 1765–1770.
35 B. Nikoobakht and M. A. El-Sayed, *Langmuir*, 2001, **17**, 6368–6374.
36 J. Fink, C. J. Kiely, D. Bethell and D. J. Schiffrin, *Chem. Mater.*, 1998, **10**, 922–926.
37 B. M. I. van der Zande, G. J. M. Koper and H. N. W. Lekkerkerker, *J. Phys. Chem. B*, 1999, **103**, 5754–5760.
38 B. M. I. van der Zande, L. Pages, R. A. M. Hikmet and A. von Blaaderen, *J. Phys. Chem. B*, 1999, **103**, 5761–5767.